

OFKE

Praktikum Angewandte Physik

Optische Festkörpereigenschaften

Dipl.-Ing. Georg Heibel<sup>1</sup>  
Institute of Solid State Physics  
Graz University of Technology  
Petersgasse 16  
A-8010 Graz

April 3, 2003

<sup>1</sup>Email: [georg.heimel@tugraz.at](mailto:georg.heimel@tugraz.at)

Tel.: +43 (0)316 873-8972

# Preface

What you are holding in your hands right now is a first version of the script that one day will accompany this lab exercise. So I would like to encourage anybody bold enough to actually read through it to report any typing and other mistakes and to comment on style and overall content of this paper. Since this is also my first L<sup>A</sup>T<sub>E</sub>X document ever, missprints are very likely to occur. This means that if anything is not clear, you don't have to change but the script will be changed to get the right message across to everybody.

The same is true for the lab exercises themselves. I am always open to new suggestions concerning materials, experimental setups, ideas for lab exercises and so on. Please do not hesitate to discuss your ideas with me. The current schedule of experiments itself is not to be concerned as more than a *beta*-version. Fortunately, the organization of the lab allows for a rather flexible compilation of experiments to be conducted. This is a great chance to do interesting physics for all of us!

My official contact coordinates are:

DI Georg HeimeI  
Institute of Solid State Physics  
Advanced Materials Division  
Graz University of Technology  
Petersgasse 16  
A-8010 Graz

Tel: 0316/873-8972  
Fax: 0316/873-8478  
EMail: georg.heimeI@tugraz.at

I usually can be found in or around room no. 311, which is on the 3<sup>rd</sup> floor of the physics building in the Solid State Physics wing.

## Topics for (recommended) further reading

In addition to the present document I would suggest (and highly recommend) to review the following topics in the textbooks listed in the Bibliography section, any other textbooks known to you and/or any lecture notes you find suitable. The information in this paper is rather condensed and is no match for the well organized style information is presented in a good textbook.

- Electrodynamics
  - plane waves
  - linear homogenous media
  - index of refraction and dielectric tensor
  - interfaces and layered media
  - reflection, transmission, absorption, Fresnel coefficients
- Solid State Physics
  - optical response
  - index of refraction and dielectric tensor
  - absorption, reflection and transmission
  - electrons in solids
  - band model for electrons (and phonons)
- (Quantum)Mechanics
  - band model of electrons and phonons
  - harmonic oscillator
  - hydrogen atom
- Optical Spectroscopy
  - light sources
  - dispersive elements and spectrometers
  - detectors

## Basic organization of the two day lab

The lab will last for two consecutive days, about 10 hours each (including breaks). We will usually start at 9 am in my office. The schedule of the lab is as follows:

- Discussion of the basics
- Experiments
  - design and setup of experiments
  - sample preparation
  - actual measurements
  - brief discussion of the results
- Closing discussion of all results
- Protocol (either individual or group)
- Discussion and (if necessary) correction of the protocols

# Contents

<b>1</b>	<b>Introduction</b>	<b>1</b>
<b>2</b>	<b>Macroscopic Description</b>	<b>2</b>
2.1	Electromagnetic Radiation . . . . .	2
2.2	Processes at interfaces . . . . .	3
2.2.1	Interfaces between transparent media . . . . .	4
2.2.2	Interfaces between transparent and absorbing media . . . . .	4
2.2.3	An absorbing slab in air . . . . .	5
2.3	Optical density . . . . .	6
2.4	The dielectric tensor $\epsilon$ . . . . .	7
<b>3</b>	<b>Microscopic Description</b>	<b>10</b>
3.1	A simple two level system - the Einstein $B$ coefficient . . . . .	10
3.2	Band structure - Electrons in crystalline solids . . . . .	12
3.3	Excitons . . . . .	17
3.4	Fluorescence . . . . .	17
3.5	Electron-Phonon coupling . . . . .	18
<b>4</b>	<b>Instrumentation</b>	<b>22</b>
4.1	Light sources . . . . .	22

4.1.1	VIS/NIR light sources . . . . .	23
4.1.2	UV light sources . . . . .	24
4.2	Optical components . . . . .	24
4.2.1	Mirrors . . . . .	25
4.2.2	Window, lenses, substrates, and sample cells . . . . .	25
4.3	Dispersive elements . . . . .	26
4.3.1	Prisms . . . . .	26
4.3.2	Gratings . . . . .	27
4.4	Detectors . . . . .	27
4.4.1	Photomultipliers . . . . .	28
4.4.2	Photoconduction detectors . . . . .	29
	<b>Bibliography</b>	<b>31</b>

# Chapter 1

## Introduction

The topic of this lab exercise are the optical properties of solids. In a broader scope, we will have to deal with the interaction of light with matter. Electromagnetic radiation covers a wide range of wavelengths where different mechanisms of interaction are important. With *optical range* one usually refers to the visible spectral range and to wavelengths right next to the visible range. More precisely, we can split the wavelengths of electromagnetic radiation that we are interested in during this lab into three parts:

- **Near Infrared (NIR)** 800nm - 10000nm
- **Visible (VIS)** 400nm - 800nm
- **Ultraviolet (UV)** 100nm - 400nm

Consequently, we will perform UV/VIS/NIR spectroscopy to investigate the optical properties of solids (and solutions). This will involve both, transmission experiments and fluorescence measurements.

This manuscript is organized as follows: First, we will discuss a macroscopic approach of light propagation in media and processes at interfaces between media. Next, we will look at the microscopic scale to explain the macroscopic quantities on the basis of the quantum mechanical nature of all matter. This not only will allow us to better understand the actual outcome of our experiments, but will also lead us to the last chapter of this document, which describes the experimental techniques and the components used to realize them. The connection to the first two, more theoretical chapters is, that the same processes that we induce and want to understand in the sample that we investigate, are exploited for applications in the measurement apparatus.

## Chapter 2

# Macroscopic Description

In this chapter we will discuss the classical electrodynamics approach to the optical response of (solid) media. Most formalisms and formulas should be already familiar to the reader. The basic concept of this approach is the propagation of light (seen as continuous electromagnetic waves rather than particles) in homogenous media and through interfaces between homogenous media.

### 2.1 Electromagnetic Radiation

For our purposes it is sufficient to regard (monochromatic) light as a linearly (say along  $x$ ) polarized plane wave of the electromagnetic field  $\mathbf{E}$  that oscillates with frequency  $\omega = 2\pi\nu$  and Amplitude  $E_0$  over time  $t$  and propagates in  $z$ -direction.

$$\mathbf{E} = E_0 e^{i(\mathbf{k}z - \omega t)} \quad (2.1)$$

Here,  $\mathbf{k}$  is the wavevector (in our case pointing in  $z$ -direction) that is related to the light wavelength  $\lambda$  and the (complex) index of refraction  $\mathbf{n}$  of the medium the light is propagating in as follows.

$$\mathbf{k} = \frac{\mathbf{n}\omega}{c} = \frac{2\pi\mathbf{n}}{\lambda} = \frac{2\pi(n + i\kappa)}{\lambda} \quad (2.2)$$

Note that the real part of  $\mathbf{n}$  (denoted as  $n$  for the rest of this document) is simply the ratio  $c/c_0$  between the speed of light  $c$  in the considered medium and the speed of light in vacuum  $c_0$ . Substituting Eq. 2.2 into Eq. 2.1 not only shows this but also reveals that the imaginary part  $\kappa$  of the refractive index describes the damping (absorption, extinction) of the electromagnetic wave inside a medium. The real part  $n$  of the refractive index is responsible for



well known phenomena like refraction or total reflection at interfaces.

$$\lambda[\text{nm}] = \frac{1239.85}{\hbar\omega[\text{eV}]} \approx \frac{1234}{\hbar\omega[\text{eV}]} \quad (2.3)$$

At this point, it seems convenient to remark that the relation between the photon energy  $\hbar\omega$  and  $\lambda$  of light is approximately given by Eq. 2.3.

## 2.2 Processes at interfaces

We will now consider a simple system (depicted in Fig. 2.1) where light with intensity  $I^0 (= \mathbf{E}\mathbf{E}^*)$  propagating in medium no. 1 characterized by  $\mathbf{n}_1$  impinges perpendicularly on the interface to a second medium described by  $\mathbf{n}_2$ .

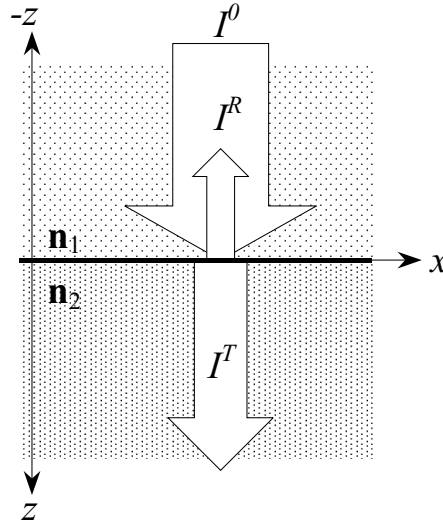


Figure 2.1: Model System of the interface between two linear, homogenous and isotropic media 1 and 2 characterized by their respective refractive index  $\mathbf{n}_1$  and  $\mathbf{n}_2$  in the reference frame of the cartesian coordinates  $x$  and  $z$ . Of the incident intensity  $I^0$  (at the interface  $z = 0$ ) one part  $I^R$  is reflected while the other part  $I^T$  is transmitted through the interface, enters medium 2 and propagates therein.

Solving Maxwell's equations for the general case depicted in 2.1 yields for the percentage of reflected light intensity:

$$\frac{I^R}{I^0} = \frac{(\mathbf{n}_1 - \mathbf{n}_2)(\mathbf{n}_1 - \mathbf{n}_2)^*}{(\mathbf{n}_1 + \mathbf{n}_2)(\mathbf{n}_1 + \mathbf{n}_2)^*} \quad (2.4)$$

Here, the star (\*) indicates the complex conjugate. Depending on the type of measurement we will conduct, there are three sample cases we need to examine more closely.

### 2.2.1 Interfaces between transparent media

We will call a medium transparent at optical wavelengths if no absorption occurs in the visible spectral range. Air, glass or water would be examples for transparent media. In our model, this means that  $\mathbf{n}_1$  and  $\mathbf{n}_2$  are real ( $\mathbf{n}_1 = n_1$  and  $\mathbf{n}_2 = n_2$ ), respectively that their imaginary parts disappear ( $\kappa_1 = 0$  and  $\kappa_2 = 0$ ). As a special case of Eq. 2.4, the percentage of reflected Intensity  $I^R$ , the *reflectivity*  $R$  and the percentage of transmitted intensity  $I^T$ , the *transmission*  $T$  are given by:

$$R = \frac{(n_1 - n_2)^2}{(n_1 + n_2)^2} \quad (2.5a)$$

$$T = 1 - R = \frac{4n_1n_2}{(n_1 + n_2)^2} \quad (2.5b)$$

Clearly, intensity that is not reflected by the interface must be transmitted through the interface ( $I^0 = I^R + I^T$ ). No loss occurs within the media.

### 2.2.2 Interfaces between transparent and absorbing media

Let us now consider the interface between a transparent medium (say air) and an absorbing medium (typically one of our samples). In that case only  $\kappa_1 = 0$  but  $\kappa_2 \neq 0$ . This means that  $\mathbf{n}_1 (= n_1)$  is real but  $\mathbf{n}_2 = n_2 + i\kappa_2$  is complex. Also, the index of refraction of air can be considered to be equal to unity, so we will assume  $n_1 = 1$ . As a further simplification of the general form presented in Eq. 2.4, the reflectivity and the transmission are then given by:

$$R = \frac{(n_2 - 1)^2 + \kappa_2^2}{(n_2 + 1)^2 + \kappa_2^2} \quad (2.6a)$$

$$T = 1 - R \quad (2.6b)$$

Again, intensity that is not reflected by the interface must be transmitted through the interface ( $I^0 = I^R + I^T$ ). But what happens to the transmitted intensity? Right after entering the absorbing medium no. 2 at  $z = 0$ ,  $I^T(z = 0) = I_0^T$  is given by Eq. 2.6. The light is then propagating in medium no. 2 in  $z$ -direction and is gradually attenuated following *Beer-Lambert's* law:

$$I^T(z) = I_0^T e^{-\alpha z}, \quad z > 0 \quad (2.7)$$

Here,  $\alpha$  is the *absorption coefficient* that is related to  $\kappa$  via:

$$\alpha = \frac{4\pi\kappa}{\lambda} \quad (2.8)$$

Light is attenuated following an exponential law in an absorbing medium.

### 2.2.3 An absorbing slab in air

Next we will consider a slightly more complex but all the more realistic system schematically depicted in Fig. 2.2. This situation corresponds more or less to that encountered in our experiments. A coplanar slab (thickness  $d$ ) of an

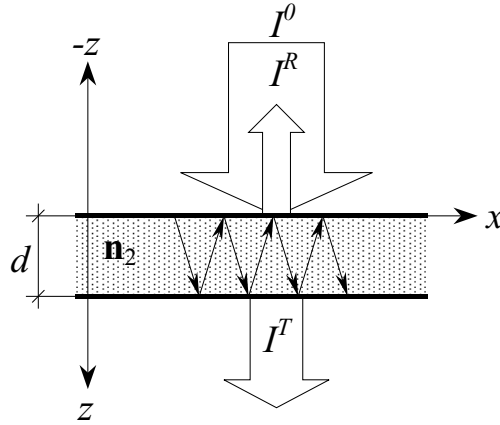


Figure 2.2: Schematic representation of a transmission experiment. The sample is a coplanar slab of thickness  $d$  of an absorbing medium ( $\mathbf{n}_2 = n_2 + i\kappa_2$ ). Reflection occurs at both interfaces, e.g. not only when light enters the slab, but also when it leaves. In total, one part of the incident intensity  $I^0$  is reflected ( $I^R$ ), one part is transmitted ( $I^T$ ) and a third part is absorbed.

absorbing medium ( $\mathbf{n}_2 = n_2 + i\kappa_2$ ) is surrounded by air ( $\mathbf{n}_1 = n_1 \simeq 1, \kappa_1 = 0$ ). In that case, multiple reflections at both interfaces and their interference have to be considered (compare Fabry-Pèrot interferometer). Provided one cannot resolve the interference fringes but rather observes an averaged value, one finds for transmission and reflectivity:

$$\langle T \rangle = \frac{(1 - R)^2 (1 + \kappa_2/n_2^2) e^{-d\alpha}}{1 - R^2 e^{-2d\alpha}} \quad (2.9a)$$

$$\langle R \rangle = R(1 + \langle T \rangle e^{-d\alpha}) \quad (2.9b)$$

In contrast to the case of a single interface discussed above, the sum of the total reflected and transmitted intensity does not equal the incident intensity

( $I^T + I^R < I^0$  unless  $\kappa_2 = 0$  as well). Part of the light ( $I^A$ ) is absorbed inside the sample so that we find  $I^T + I^R + I^A = I^0$ . To really determine the complex refractive index of a material would be a major experimental task, that requires elaborate and quite involved techniques (*ellipsometry*).

## 2.3 Optical density

For our experiments we will somehow simplify and modify above described situation, because there are certain limitations we have not discussed yet.

- In general, our samples do not form freestanding films. They have to be investigated mounted on a supporting (glass-)substrate making the total system one of three media (air-sample-substrate-air) and three interfaces.
- We do not know the exact thickness of the layer of sample material.
- Reflectivity is harder to measure since it involves more optical components that need to be accounted for. Therefore we will mainly conduct transmission experiments, where we know  $I^0$  and experimentally determine  $I^T$ .
- For soluble systems we need to consider the system air-vial-solvent-sample where above findings can not be applied that easily.

Therefore we will consider neither the refractive index nor the absorption coefficient but a third quantity, the *optical density* (OD). In order to motivate the term optical density we consider the way we will measure it.

1. Determine the transmission of the substrate (or solvent in vial) alone.
2. Measure the transmission of sample plus substrate (or solvent).
3. Neglect the differences in the reflection processes in the two measurements. All that remains to be considered is then the difference in the absorption processes in the two measurements.

Suppose the intensity transmitted through the substrate alone is  $I_{substrate}^T$  and the intensity transmitted through the system sample+substrate is  $I_{sample}^T$ . We then propose (compare Eq. 2.7) the relation:

$$I_{sample}^T = I_{substrate}^T e^{-\alpha d} \quad (2.10)$$

where  $d$  is the thickness of the sample layer (see Fig. 2.2). Since we do not know the thickness of the sample we can only extract the product  $\alpha d$  and define

the optical density as:

$$T = \frac{I_{sample}^T}{I_{substrate}^T} = e^{-\alpha d} \quad (2.11a)$$

$$OD = -\log_{10} \left( \frac{I_{sample}^T}{I_{substrate}^T} \right) = -\log_{10}(T) \propto \alpha d \quad (2.11b)$$

For example  $OD = 1$  means that only one tenth of the light is transmitted through the sample *and* the substrate compared to the substrate alone (transmittance  $T = 0.1 = 10\%$ ).

## 2.4 The dielectric tensor $\epsilon$

While the refractive index  $\mathbf{n}$  is the quantity dealt mostly with in optics, the real material related quantity that appears in Maxwell's equations is the *dielectric function* (tensor)  $\epsilon$ . It describes the (linear) response of a substance to an external electric field  $\mathbf{E}_{ext}$ . In our case this (time dependent) external electric field is of the form Eq. 2.1. By polarizing the medium (shifting the electrons with respect to their nuclei and thus creating dipoles and dipole moments) a field opposite to the external one is generated inside the sample. We call this the macroscopic *polarization*  $\mathbf{P}$ . The resulting field inside the material,  $\mathbf{E}_{int}$ , is then simply the sum of  $\mathbf{E}_{ext}$  and  $\mathbf{P}$ .

$$\mathbf{E}_{int} = \mathbf{E}_{ext} + \mathbf{P} \quad (2.12)$$

In general,  $\mathbf{P} = \mathbf{P}(\mathbf{E})$  will be some function of the electric field, in our case it is simply proportional. The constant factor relating polarization to electric field is the electric *suszeptibility*  $\chi$ . The dielectric function is related to  $\chi$  via:

$$\mathbf{E}_{int} = \mathbf{E}_{ext} + \chi \mathbf{E}_{ext} = (1 + \chi) \mathbf{E}_{ext} = \epsilon \mathbf{E}_{ext} \quad (2.13a)$$

$$\epsilon = 1 + \chi \quad (2.13b)$$

In the same way as  $\mathbf{n}$  can be conveniently denoted as a complex quantity, also  $\epsilon = \epsilon_r + i\epsilon_i$  is complex in general with a real part  $\epsilon_r$  and an imaginary part  $\epsilon_i$ . The relation between the dielectric function and the refractive index is:

$$\mathbf{n} = \sqrt{\epsilon} \quad (2.14)$$

Since both quantities are complex we find for the real and imaginary parts the relations

$$n = \frac{1}{\sqrt{2}} \sqrt{\epsilon_r + |\epsilon|} \quad (2.15a)$$

$$\kappa = \frac{1}{\sqrt{2}} \sqrt{-\epsilon_r + |\epsilon|} \quad (2.15b)$$

on one hand and solving for  $\epsilon$  we find

$$\epsilon_r = n^2 - \kappa^2 \quad (2.16a)$$

$$\epsilon_i = 2n\kappa \quad (2.16b)$$

on the other hand. If  $\epsilon_i \neq 0$  the external electric field not only polarizes the medium but also induces a current to flow, like one would expect it to be the case for conducting media. The imaginary part of the dielectric function is then related to the (optical) conductivity  $\sigma$  of the investigated materials via

$$\epsilon_i = \frac{\sigma}{\epsilon_0 \omega} \quad (2.17)$$

where  $\epsilon_0$  is the vacuum dielectric constant and  $\omega$  the light frequency (see Eqs. 2.1 and 2.2).

The dielectric tensor is above all a function of the frequency of the incident light. Its real and imaginary parts are not independent of each other. They are linked via a so called *Kramers-Kronig* relation.

$$\epsilon_r = \epsilon_r(\infty) + \frac{2}{\pi} \int_0^\infty \frac{\omega' \epsilon_i(\omega')}{\omega'^2 - \omega^2} d\omega' \quad (2.18a)$$

$$\epsilon_i = \frac{2\omega}{\pi} \int_0^\infty \frac{\epsilon_r(\omega') - \epsilon_r(\infty)}{\omega'^2 - \omega^2} d\omega' \quad (2.18b)$$

Here,  $\epsilon_r(\infty) \simeq 1$  is the real part of the dielectric function far of from any resonance (=absorption) at very short light wavelengths. It arises from the response of the (positively charged) nuclei in the solid to the external (time-dependent) electric field. We will now try to visualize the Kramers-Kronig equations. From Eq. 2.15 follows that if  $\epsilon_i = 0$  then also  $\kappa = 0$  which means that the medium does not absorb. However, if  $\epsilon_i = 0$  for any  $\omega$  then  $\epsilon_r(\omega) = \epsilon_r(\infty) \simeq 1$ . This would lead to an  $n \simeq 1$  (via Eq. 2.15) and therefore to a medium that not only does not absorb but also does not refract or show any particular optical response different from vacuum. From Eq. 2.18 follows that only in the vicinity of an absorption feature ( $\epsilon_i > 0$ ) the real part  $\epsilon_r$  is different from  $\epsilon_r(\infty)$ . More precisely  $\epsilon_r > \epsilon_r(\infty)$  right below an absorption feature and  $\epsilon_r < \epsilon_r(\infty)$  right above (see Eq. 2.18). This behavior is schematically represented in Fig. 2.3.

The real significance of the the Kramers-Kronig relations is that they allow to compute one part of the dielectric function when only the other is known from experiment. The major difficulty to overcome here are the boundaries of the integrals in Eq. 2.18. In a typical realistic situation, the "known" part of the dielectric function has only been measured in a limited energy range of the light (for instance in the UV/VIS/NIR), which normally is far from  $[0, \infty)$ .

To round off this chapter, the optical constants of some important substances are listed in Tab. 2.1.

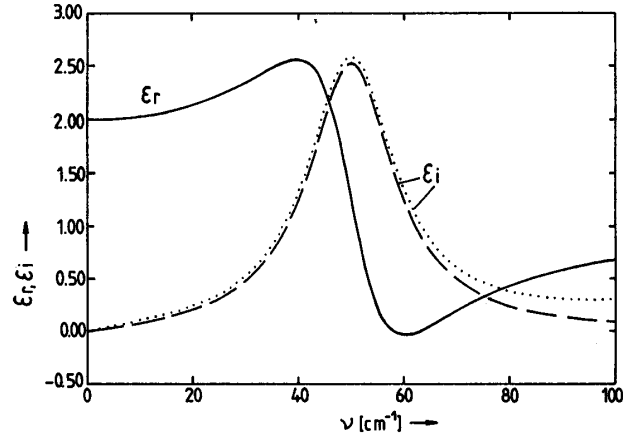


Figure 2.3: Real ( $\varepsilon_r$ , solid line) and imaginary ( $\varepsilon_i$ , dashed line) part of a model dielectric function as a function of the wavenumber  $\bar{\nu}$  (in  $\text{cm}^{-1}$ ). The dotted line is  $\varepsilon_i$  calculated from  $\varepsilon_r$  using the Kramers-Kronig relations (Eq. 2.18).

Table 2.1: Real part of the index of refraction ( $n$ ), its imaginary part ( $\kappa$ ), and the absorption coefficient ( $\alpha$ ) of several important materials. The wavelength ( $\lambda$ ) these quantities were measured at is also given.

Material	$n$	$\alpha[\text{cm}^{-1}]$	$\kappa$	$\lambda[\text{nm}]$
Quarz-Glas	1.45800	-	-	589.3
Polyethylene	1.51000	-	-	589.3
$\text{Al}_2\text{O}_3$	1.77380	-	-	589.3
Diamond	2.46000	0.10	-	400.0
GaAs	4.04000	-	-	546.1
Silicon	4.20000	$3 \cdot 10^3$	-	589.0
Germanium	5.10000	$1 \cdot 10^4$	-	1000.0
NaCl	1.54414	-	-	589.0
Silver	0.18100	-	3.67	589.0
Aluminum	1.44000	-	5.23	589.0
Water (20°C)	1.33283	-	-	589.3
Toluene (20°C)	1.49693	-	-	589.3

## Chapter 3

# Microscopic Description

So far we have learned how absorption and extinction processes in solids affect their optical response and how to describe the optical properties of media with macroscopic constants that fit well into the nice theory of electrodynamics based on Maxwell's equations. The origin of all light-matter interaction has of course to be searched on the microscopic scale. Any matter is, after all, a bunch of (negatively charged) electrons whirling around some more or less fixed, heavy, and positively charged nuclei. On the length and energy scales where we can observe nuclei, electrons and the distances and binding energies between them, classical models break down and one has to resort to quantum mechanics. In this chapter we will devise models to describe the interaction of light (still seen as an electromagnetic wave) with simple quantum mechanical model systems. A crosslink from the microscopic processes, that are of essentially quantized nature, to the classical, macroscopic material constants will be established.

### 3.1 A simple two level system - the Einstein $B$ coefficient

Any system consisting of electrons and nuclei, be it a single atom, a molecule or a solid, has a quantum mechanical ground state and an (or several) excited state(s). Under certain conditions, that we will discuss in this section, the system in question can undergo a transition between these states. We will assume that the system resides in its ground state  $|\Psi_0\rangle$  with the ground state energy  $E_0$  before we shine light on it. Furthermore we will consider one single excited state  $|\Psi_1\rangle$  with energy  $E_0 + \hbar\omega_{01}$  only. The whole system is now that



of a medium represented by two states and a (monochromatic) continuous light wave with frequency  $\omega$  that is switched off for times  $t < 0$  and switched on for  $t > 0$ . The situation for  $t < 0$  and immediately after switching on the light are schematically represented in Fig. 3.1(a) and 3.1(b). With a certain probability,

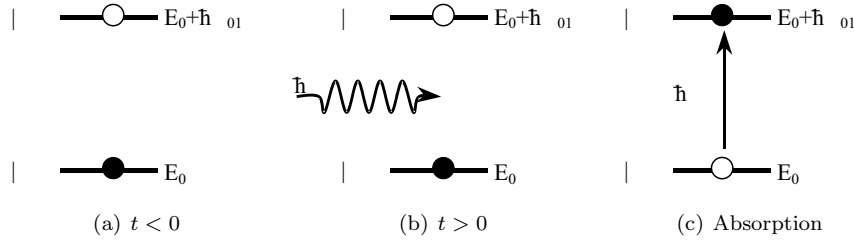


Figure 3.1: The quantum mechanical test system is in its ground state  $|\Psi_0\rangle$  before the light is switched on (a). For times  $t > 0$  light with frequency  $\omega$  is allowed to interact with (the electrons of) the system (b). This may lead to the absorption of an energy quantum  $\hbar\omega_{01}$  out of the electromagnetic field that promotes the system from  $|\Psi_0\rangle$  into its first excited state  $|\Psi_1\rangle$  (c).

the system now takes up one quantum  $\hbar\omega_{01}$  of light from the electromagnetic field it is interacting with. After this absorption process, the system is no longer in its ground state  $|\Psi_0\rangle$ , but rather in its first excited state  $|\Psi_1\rangle$ . Mind that it is still interacting with the light field. This situation is depicted in Fig. 3.1(c). For an atom or molecule, this process corresponds to promoting an electron from the highest occupied orbital into the lowest energy unoccupied orbital.

A realistic medium might be considered as an ensemble of very many such two level systems (atoms, molecules, ...). Let us assume the number of two level systems in their ground state per unit volume (density) to be  $n_0$ . The number of absorption processes per time and volume is then given by:

$$\frac{dn_0}{dt} = -B_{01}n_0u_\omega f(\omega) \quad (3.1)$$

where  $u_\omega$  is the spectral density of the light,  $f(\omega)$  the normalized lineshape of the transition and  $B_{01}$  the *Einstein B coefficient* for absorption. The spectral density of the incident light is equal to the number of photons of frequency  $\omega$  per unit cell volume. In the case of monochromatic light this reduces to a delta function  $\delta_\omega$ . The lineshape  $f(\omega)$  of the transition accounts for the fact that light is not only absorbed if the light frequency matches the transition frequency exactly ( $\omega = \omega_{01}$ ) but also if it is close by. Only the transition probability is much lower. This can be motivated by a kind of energy-time uncertainty relation. As we will see later (see Sect. 3.4) the two level system does not stay forever in its excited state but relaxes back down. The time it

stays up in  $|\Psi_1\rangle$  determines the width  $\Gamma$  of the absorption line. The lineshape is usually described by a *Lorentz* profile (see Eq. 3.2) very much like in a damped and forced harmonic oscillator.

$$f(\omega) = \frac{2}{\pi} \frac{\Gamma}{4(\omega - \omega_{01})^2 + \Gamma^2} \quad (3.2)$$

The Einstein  $B$  coefficient can be derived from time dependent perturbation theory in quantum mechanics. The result is:

$$B_{01} = \frac{4\pi^2\beta}{\hbar e^2} \sum_{\xi} |\langle \Psi_1 | \hat{\mu}_{\xi} | \Psi_0 \rangle|^2 \quad (3.3)$$

where the sum runs over all cartesian components  $\xi$  of the electric dipole operator  $\hat{\mu}$  (related to the position operator  $\hat{\mathbf{r}}$  via  $\hat{\mu} = -e\hat{\mathbf{r}}$ ) and  $\beta$  is the fine structure constant:

$$\beta = \frac{e^2}{4\pi\epsilon_0\hbar c} \simeq \frac{1}{137} \quad (3.4)$$

with the elementary charge  $e$ . The absorption coefficient (see Eq. 2.8) is related to this Einstein  $B$  coefficient and Eq. 3.1 via:

$$\alpha \propto \hbar\omega_{01} B_{01} \quad (3.5)$$

since Eq. 2.7 is for intensities and Eq. 3.1 is for numbers of events. Note that integrating Eq. 3.1 under consideration of Eq. 3.5 yields Eq. 2.7.

## 3.2 Band structure - Electrons in crystalline solids

The two level system is a good description for gases and liquids, where the isolated two level systems correspond to atoms or molecules that do not interact too much with each other. In both cases, the microscopic constituents of the system are arranged randomly and change their positions and orientations relative to each other due to thermal motion. However, in many solids, the atoms and molecules interact more strongly and arrange in perfectly regular, periodic patterns. This periodicity, the long range order, and the interaction between the building blocks are responsible for some particular properties of the electronic states in crystalline solids. The ground and excited states  $|\psi_0^i\rangle$  and  $|\psi_1^j\rangle$  of the originally decoupled two level systems start to interact and form new states.

Let us first consider the simplest case of two interacting units 1 and 2 with the ground (occupied) states  $|\psi_0^1\rangle$  and  $|\psi_0^2\rangle$  and the excited (unoccupied) states  $|\psi_1^1\rangle$  and  $|\psi_1^2\rangle$  respectively. The corresponding energies are  $E_0^1 = E_0^2$  and  $E_1^1 = E_1^2$ . Furthermore, we will assume that in the ground states of each of the

units there are two electrons, one with spin up ( $\uparrow$ ) and one with spin down ( $\downarrow$ ). At large distance the two systems do not interact (left and right edge in Fig. 3.2). When bringing the units close together, they start to interact and form new states  $|\psi_0^+\rangle$ ,  $|\psi_0^-\rangle$ ,  $|\psi_1^+\rangle$ , and  $|\psi_1^-\rangle$  that are related to the  $|\psi_0^i\rangle$  and  $|\psi_1^j\rangle$  via:

$$|\psi_0^\pm\rangle = \frac{1}{\sqrt{2}} (|\psi_0^1\rangle \pm |\psi_0^2\rangle) \quad (3.6a)$$

$$|\psi_1^\pm\rangle = \frac{1}{\sqrt{2}} (|\psi_1^1\rangle \pm |\psi_1^2\rangle) \quad (3.6b)$$

The energies of these new states,  $E_0^\pm$  and  $E_1^\pm$  are in general different from each other and from the  $E_0^i$  and  $E_1^j$  of the non-interacting system (center in Fig. 3.2). This also implies that the new transition energy  $\hbar\omega_{01}^\mp$  of the interacting system is different (smaller) than  $\hbar\omega_{01}$  of the non-interacting system. The form of the wavefunctions is only schematically indicated to emphasize that they will in general be different for ground (occupied) and excited (unoccupied) states. Exciting the system from its ground state to its first excited state corresponds

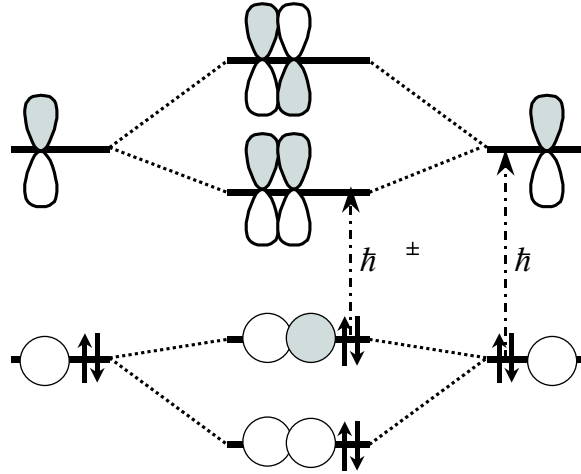


Figure 3.2: Two systems characterized by a ground state  $|\psi_0\rangle$  with two electrons in it and an (unoccupied) excited state  $|\psi_1\rangle$  start to interact at low distances. New occupied and unoccupied levels  $|\psi_0^+\rangle$ ,  $|\psi_0^-\rangle$ ,  $|\psi_1^+\rangle$ , and  $|\psi_1^-\rangle$  are created as linear combinations of the non interacting levels. Orbital energies and excitation energies  $\hbar\omega_{01}$  change due to the interaction.

to promoting an electron from the **h**ighest **o**ccupied **m**olecular **o**rbital (*HOMO*) into the **l**owest **u**noccupied **m**olecular **o**rbital (*LUMO*).

At the next level of theory we will consider an infinite linear chain of two level systems that are separated by a distance  $a$ . The ground states  $|\psi_0^i\rangle$  and

excited states  $|\psi_1^j\rangle$  again interact and form new states. Instead of a simple *plus* and *minus* linear combination (see Eq. 3.6) as in the two subsystem case, we will now have a whole range of phase relations between neighboring systems. This situation is depicted in Fig. 3.3 for both, occupied and unoccupied states. Again, the form of the wavefunction on the individual sites has no physical justification. It has been chosen simply to visualize the relation between the amplitude and the sign of the wavefunctions on different sites. From top to

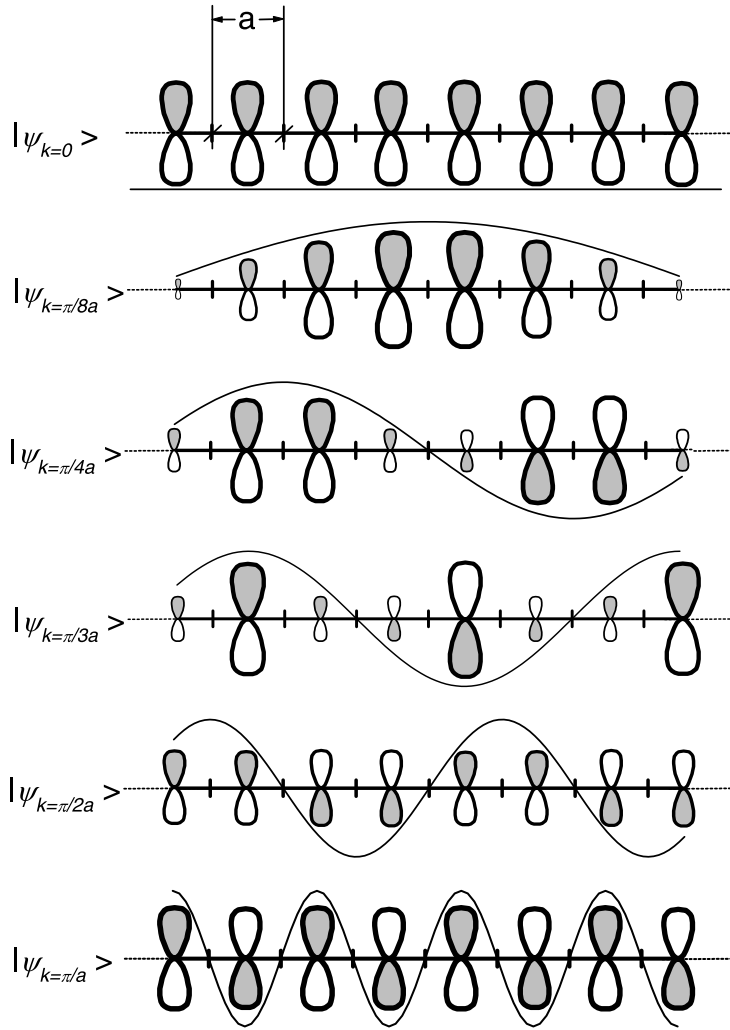


Figure 3.3: In a linear chain of interacting two level systems separated by a distance  $a$ , the wavefunctions of both the ground (occupied) and the excited (unoccupied) states mix and form new wavefunctions  $|\psi_k\rangle$  with a certain lattice periodicity characterized by the wavevector  $k$ .

bottom in Fig. 3.3 we see a few possible wavefunctions  $|\psi_k\rangle$  between the two

extremals where all repeating units look alike (top panel) and where the wavefunctions in adjacent subsystems are of opposite sign (bottom panel). These wavefunctions  $|\psi_k\rangle$  are characterized by a lattice periodic part  $u_k(x)$  (related to  $|\psi_0\rangle$  or  $|\psi_1\rangle$ ) but not necessarily equal to, as falsely implicated in Fig. 3.3) and a certain  $k$  that specifies their periodicity with respect to the periodicity of the lattice  $a$ . The pictorial approach from Fig. 3.3 can be formulated mathematically as:

$$\psi_k(x) = u_k(x)e^{-ikx} \quad (3.7)$$

Such functions (Eq. 3.7) are called *Bloch* functions. Generally, the energy of a given  $|\psi_k\rangle$  depends on  $k$ . In the case of almost free electrons the energy dispersion relation is of the functional form:

$$E(k) = \frac{\hbar^2 k^2}{2\mu_{eff}} \quad (3.8)$$

where  $\mu_{eff}$  is the effective mass of an excess electron in an unoccupied (excited) state ( $\mu_e > 0$ ) or the effective mass of an excess hole in one of the occupied (ground) states ( $\mu_h < 0$ ). When we plot the state energies as a function of the

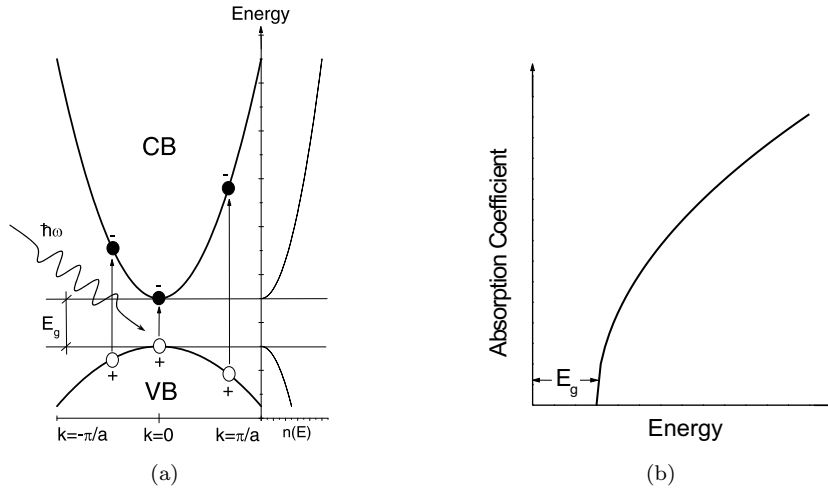


Figure 3.4: In the left panel (a) the valence (VB) and conduction band (CB) for the case of quasi-free electrons in a semiconductor with gap energy  $E_g$  are plotted. Right next to the band scheme the density of states  $n(E)$  is given. The vertical arrows represent optical transitions where an electron is excited from the VB to the CB by absorbing light  $\hbar\omega$ . These inter-band transitions result in an energy dependent absorption coefficient  $\alpha$  plotted in the right panel (b).

wavevector, we arrive at the so called *bandstructure* of our model system (see Fig. 3.4), where the occupied states derived from the two-level ground state  $|\psi_0\rangle$  form the *valence band* (VB) and those stemming from the  $|\psi_1\rangle$ s evolve

towards the *conduction band* (CB). If the former is fully occupied and does not energetically overlap with the latter the considered material is an isolator. If the forbidden energy window is small enough to be in the optical region, isolators are commonly called semiconductors and the forbidden energy window is the *bandgap*. The bandgap energies  $E_g$  for some important semiconductors are listed in Tab. 3.1. In a realistic 3D crystal, the form of the bands will be different for each direction and  $k$  will become a vector  $\mathbf{k}$ . However, for a polymer the 1D bandstructure model is still under discussion.

Table 3.1: Bandgap energies in eV at room temperature for some important semiconductors

Material	$E_g[\text{eV}]$
Si	1.120
Ge	0.665
GaAs	1.430
PbS	0.370
InSb	0.180

If we review Eqs. 3.1 to 3.5 we can conclude that in addition to our Lorentzian lineshape, the absorption coefficient  $\alpha$  becomes energy dependent. For any given light energy  $\hbar\omega$  there is a number of occupied-unoccupied state pairs distributed over  $\mathbf{k}$ -space. How many states there are at a certain energy is determined by the *density of states* (DOS). The probability for an absorption process will certainly be proportional to that. Since the photon momentum is much smaller than the electron momentum, only vertical transitions need to be considered as indicated in Fig. 3.4(a). Consequently, for any given transition energy, we need to sum over all  $\mathbf{k}$  and over all corresponding pairs of initial (occupied) and final (unoccupied) states that match the energy in question. Expanding Eq. 3.3 accordingly yields for the respective Einstein  $B_{eh}$  (*electron-hole*) coefficient:

$$B_{eh}(\omega) \propto \sum_{\xi} \sum_{\mathbf{k}} |\langle \psi_{\mathbf{k}}^{VB} | \hat{\mu}_{\xi} | \psi_{\mathbf{k}}^{CB} \rangle|^2 \delta(E(\mathbf{k})^{CB} - E(\mathbf{k})^{VB} - \hbar\omega) \quad (3.9)$$

The cartesian components of the Einstein  $B_{eh}$  coefficient and subsequently the absorption coefficient and the dielectric tensor can be obtained by omitting the sum over the cartesian orientations  $\xi$ . A number of further simplifications to Eq. 3.9 finally leads to a square root dependence of the absorption coefficient on the incident light energy, as depicted in Fig. 3.4(b).

### 3.3 Excitons

As discussed in the last section, light with energy greater than the bandgap promotes an electron from the fully occupied valence band into the completely empty conduction band. However, the electron and the hole do not move independently from each other, once they are generated. Since the hole represents a positive charge and the electron a negative charge, one would expect the two to interact via Coulomb attraction. This is indeed the case in many anorganic and organic semiconductors. The two charges form a hydrogen-atom-like system. Instead of one completely delocalized electron and a delocalized hole, the primary optical excitation in semiconductors is a bound electron-hole pair called *exciton*.

This exciton is localized in space and its energy is smaller than the gap energy  $E_g$  by the *exciton binding energy*. The consequences of this localization are further discussed in Sect. 3.5.

### 3.4 Fluorescence

So far, we have only considered light absorption processes, where energy is transferred from the electromagnetic field into our absorbing entity. This results either in promoting a two level system from its ground to an excited state or, in the case of semiconductors, in the promotion of an electron from the valence to the conduction band. The latter process corresponds to the creation of an exciton. The system does not stay forever in its excited state. After a certain lifetime  $\tau$  it relaxes back to the ground state, the electron and the hole recombine by emitting a photon.

Let us again consider a (disordered) ensemble of (non-interacting) two level systems. We start off with a certain amount (represented by a density  $n_1$ ) of the systems being in their excited state  $|\Psi_1\rangle$  as shown in Fig. 3.1(c) and the rest still being in their ground state  $|\Psi_0\rangle$ . We then switch off the light and let the system evolve. The change in the density of systems in their excited state with time will follow a certain natural rate equation:

$$\frac{dn_1}{dt} = -A_{10}n_1 \quad (3.10)$$

where  $A_{10}$  is the *Einstein A coefficient* for spontaneous emission. It can be shown that it is related to the Einstein B coefficient via:

$$\frac{A_{10}}{B_{01}} = \frac{2}{\pi} \frac{1}{\hbar^2 c^3} (\hbar\omega_{01})^3 \quad (3.11)$$

If one compares this finding to Eq. 3.3, one realizes that the one crucial quantity that relates the microscopic electronic structure of our system to the macroscopic, experimentally observable effects, is the matrix element of the electric dipole operator between the ground and the excited state of the system. This is true for absorption *and* emission processes. Integrating Eq. 3.10 yields an exponential decay law with a lifetime of the excited state  $\tau^{-1} = A_{10}$ .

Fluorescence cannot only come from isolated two level systems, but also from solids. But if we consider the band model of the solid presented in Sect. 3.2, what is the initial, excited state, and what is the final state, the ground state? For our sample semiconductor, the ground state is the fully occupied valence band with an empty conduction band. In a free electron-hole pair, the two charges are independently delocalized over the whole sample. However, for recombination, they need to be physically close to each other, as is the case in an exciton. Mind that, like a hydrogen atom, an exciton also knows excited states. However, *Kasha's rule* states that a system, once excited, relaxes quasi instantaneously into its lowest energy excited state from whence all fluorescence comes from. Consequently, one can photoexcite a semiconductor with any light of energy greater than  $E_g$  minus the exciton binding energy, but fluorescence will always come from the lowest lying exciton state. The emission light frequency is independent of that used for excitation. It is only determined by the electronic structure of the sample in question and is thus a characteristic quantity of the material.

### 3.5 Electron-Phonon coupling

So far, we have completely neglected the fact that the configuration of the electrons between the nuclei affects the binding between them. Suppose the nuclei of a molecule or a solid to be at their equilibrium positions and the electron cloud surrounding them to be in its ground state. The chemical bonds between the individual atoms, that is the equilibrium distance between atoms and the restoring force acting when displacing atoms out of their equilibrium positions, are solely determined by that electron cloud. By photoexciting the system and thus creating a bound electron-hole pair, one locally changes the electron configuration on and between nuclei. This will change the nature of the chemical bond between the nuclei in the vicinity of this electronic excitation. One can expect that as a consequence other equilibrium positions of the concerned nuclei would be optimal for the system (lower energy). Forces will act on the concerned nuclei and push them towards their new equilibrium positions in the excited state. This will not only stabilize the exciton by lowering its energy but also further



confine and localize it. Following Kasha's rule, fluorescence will then start from this relaxed excited state back towards the ground state. So fluorescence will in general be red shifted with respect to the lowest energy absorption. The above described situation is depicted in Fig. 3.5.

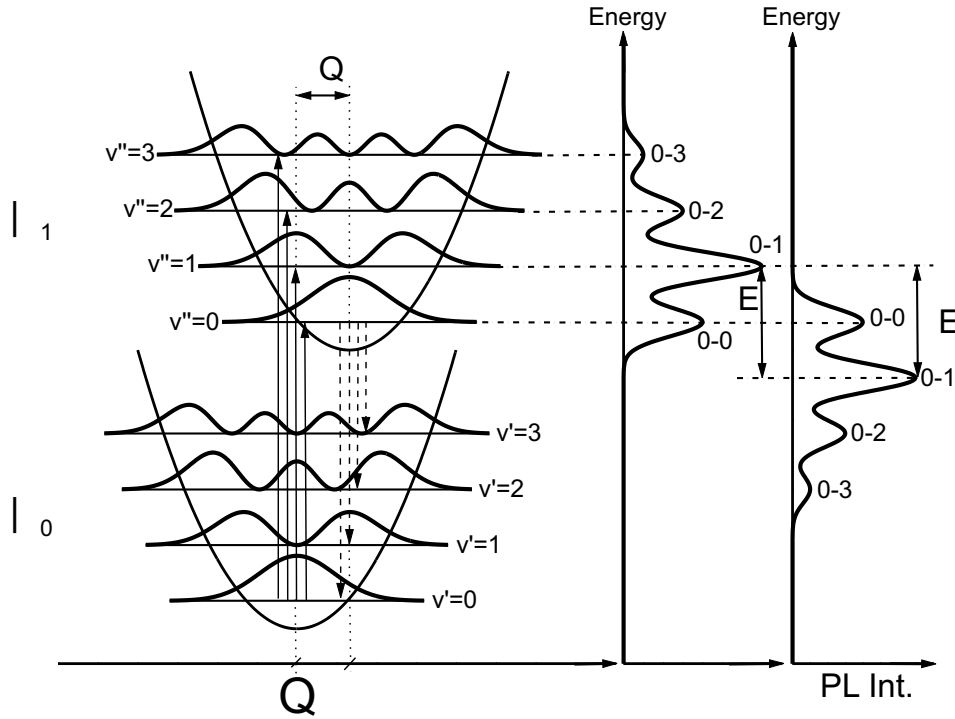


Figure 3.5: In addition to the electronic ground and excited state  $|\psi_0\rangle$  and  $|\psi_1\rangle$ , we introduce vibrational wavefunctions characterized by their quantum number  $v'$  and  $v''$  respectively. The energy parabola are chosen to describe the vibrational motion and relaxation ( $\Delta Q$ ) along one normal coordinate  $Q$  of the system. The upwards arrows indicate allowed absorption transitions, the downward arrows represent allowed emission transitions. The considered transitions lead to the observed energy dependence of the absorption coefficient  $\alpha$  (middle panel) and to the energy distribution of photoluminescence intensity (PL int., right panel). The resulting energy difference between the maxima of absorption and emission spectra  $\Delta E$  is referred to as *Stokes Shift*.

Before the absorption process, the system is in its electronic ground state  $|\psi_0\rangle$ . All nuclei reside at their respective equilibrium position  $Q = 0$ . More precisely they vibrate with a frequency  $\Omega$  around their equilibrium position in a harmonic oscillator potential with a zero point energy of  $\frac{1}{2}\hbar\Omega$ . In other words, the system is not only in its electronic ground state, but also in the respective

vibronic ground state  $|v' = 0\rangle$  or simply  $|0'\rangle$ . The total wavefunction of the system is the product  $|\psi_0\rangle|0'\rangle$  of the electronic and the vibronic parts (*Born-Oppenheimer* approximation). In the excited state, the equilibrium distance between the concerned nuclei is different ( $\Delta Q$ ) and therefore also the vibronic part of the excited state total wavefunction  $|\psi_1\rangle|v''\rangle$ . In order to evaluate our energy dependent absorption coefficient  $\alpha(\omega)$  we need to consider not one but many final states  $|\psi_1\rangle|v'' = 0, 1, 2, \dots\rangle$  for the matrix element of the electric dipole operator between initial (ground) and final state.

$$\langle 0' | \langle \psi_0 | \hat{\mu}_\sigma | \psi_1 \rangle | v'' \rangle = \overbrace{\langle \psi_0 | \hat{\mu}_\sigma | \psi_1 \rangle}^{elec.} \underbrace{\langle 0' | v'' \rangle}_{vib.} \quad (3.12)$$

As indicated in Eq. 3.12, the electric dipole operator acts only on the electronic part of our wavefunctions. Consequently the vibrational part can be separated and reduces to calculating the overlap  $\langle 0' | v'' \rangle$  between the vibrational wavefunctions in the electronic ground and excited state. The electronic absorption crosssection (treated in Sect. 3.1) is redistributed among the different vibrational transitions  $|0'\rangle \rightarrow |v''\rangle$ . In Fig. 3.5, the two vibrational energy parabolas are displaced along  $Q$  by an amount  $\Delta Q$ . The maximum of  $|0'\rangle$  is vertically aligned with the left maximum of  $|1''\rangle$  as indicated by the left vertical dotted line. We can therefore expect  $\langle 0' | 1'' \rangle$  to be the most important overlap matrix element and consequently the  $|0'\rangle \rightarrow |1''\rangle$  transition to be the most prominent in the absorption spectrum of our model system (0-1 in the middle panel of Fig. 3.5).

Once the system is excited and has arrived in its upper state  $|\psi_1\rangle|v''\rangle$ , it relaxes ultrafastly into its lowest energy excited state  $|\psi_1\rangle|0''\rangle$  (Kasha's rule). There it stays for the excited state lifetime  $\tau$  and then drops back to the electronic ground state by emitting a photon. Again, the system can drop back to any vibrational state  $|v'\rangle$  of the electronic ground state  $|\psi_0\rangle$ . How the photoluminescence (PL) intensity is redistributed among the possible transitions depends again on the overlap matrix elements  $\langle v' | 0'' \rangle$ . Since the harmonic oscillator vibrational energy parabolas in Fig. 3.5 have the same curvature, the situation is symmetrical to the absorption process. The maximum of  $|0''\rangle$  is vertically aligned with the right maximum of  $|1'\rangle$  as indicated by the right vertical dotted line. We can therefore expect  $\langle 1' | 0'' \rangle$  to be the most important overlap matrix element and consequently the  $|0''\rangle \rightarrow |1'\rangle$  transition to be the most prominent in the fluorescence spectrum of our model system (0-1 in the right panel of Fig. 3.5).

In contrast to our simple two level model (Sects. 3.1 and 3.4), where the maxima of absorption and emission spectrum (Lorentz profiles as in Eq. 3.2) are at the same energy, the maxima of absorption and emission spectrum are now energetically displaced by a  $\Delta E$ , referred to as *Stokes shift* hereafter. The

overall shape of the absorption and emission spectra, that is the relative intensity of the  $|v'\rangle \leftrightarrow |v''\rangle$  transitions, is determined by  $\Delta Q$ . In Fig. 3.6, the relative intensity of the vibronic transitions is shown for a different values of  $\Delta Q$ .

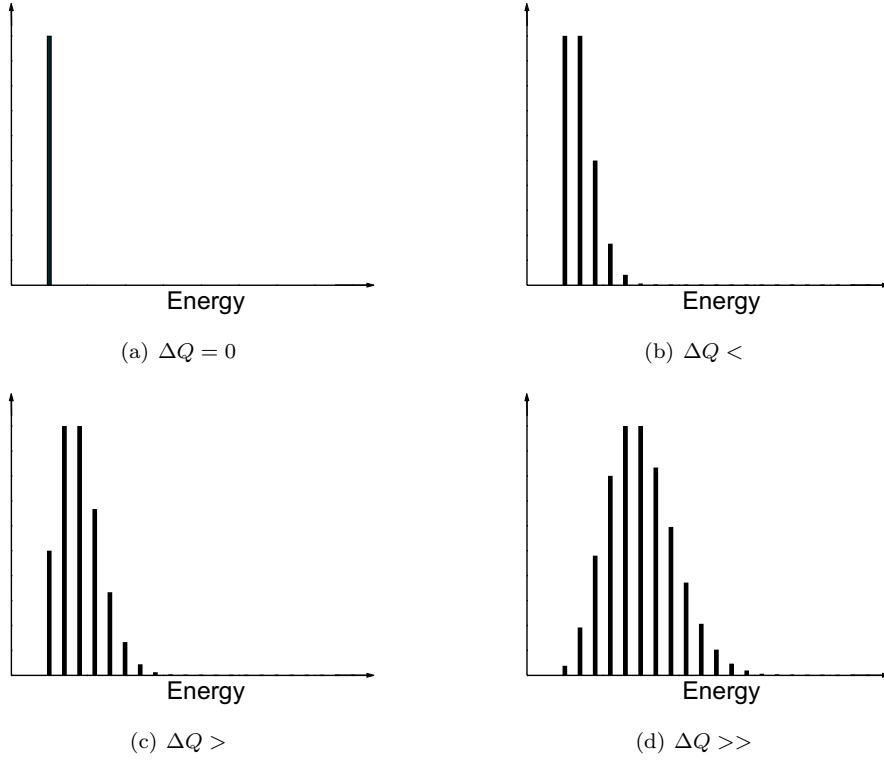


Figure 3.6: The redistribution of the electronic oscillator strength among the vibronic transitions depends on the displacement of the ground and excited state energy parabola along some normal coordinate  $Q$ . At  $\Delta Q = 0$  (a) all oscillator strength is concentrated into the 0-0 transition, all others are forbidden. For  $\Delta Q \neq 0$  (b-d) transitions to higher and higher vibrational states borrow from the intensity of the electronic transition. The total spectral feature gets broader and broader.

## Chapter 4

# Instrumentation

In this chapter, a short description of the experimental techniques, setups and components necessary to do actual measurements will be given. Let us consider the basic building blocks of a spectroscopic experiment:

- Light Source
- Optical Components
- Dispersive Element
- Detector

Since the instrumentation is practically the same for transmission and fluorescence measurements, the layout of this chapter will follow above list.

### 4.1 Light sources

Depending on the media and the principles used to create illumination, we can divide light sources into two main groups. One for the VIS/NIR region and one for the UV region. Many spectrometers have installed one of each type of lamp in order to cover the whole spectral range needed in UV/VIS/NIR spectroscopy. This generally involves switching of the light sources at a certain point during the measurement.

### 4.1.1 VIS/NIR light sources

The conceptually most simple method of illumination is the use of *black body radiation* where the temperature  $T$  of the source determines the spectral emission characteristic following *Planck's law*.

$$E(\lambda) = \frac{2hc^2}{\lambda^5} \frac{1}{e^{\frac{hc}{\lambda k_B T}} - 1} \quad (4.1)$$

Here,  $\lambda$  is the wavelength of the emitted light,  $h$  is Planck's constant, and  $k_B$  Boltzmann's constant. The actual black body emitter is usually a metal (tungsten) heated ohmically. The form of the emitted spectrum (Eq. 4.1) is shown in Fig. 4.1.

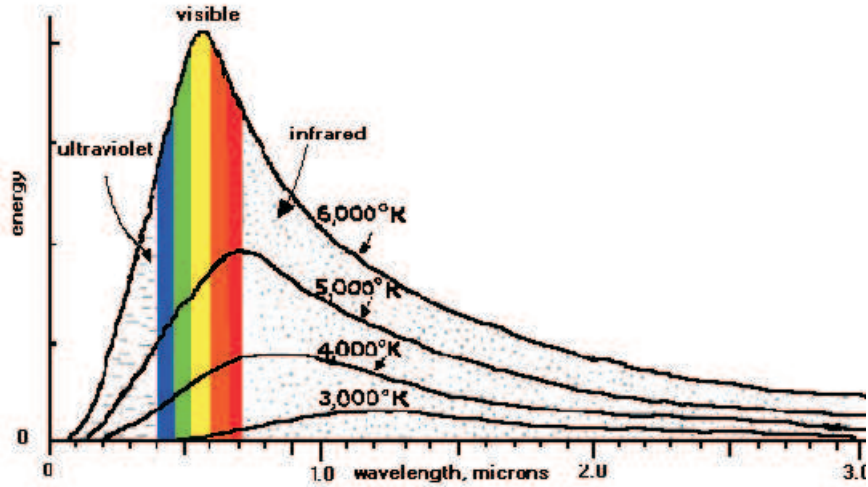


Figure 4.1: Emitted light intensity of a black body as a function of wavelength. The curve parameter is the temperature of the source.

The one wavelength  $\lambda_{max}$  where the maximum intensity is emitted is given by *Wien's law*.

$$\lambda_{max}T = \text{const.} = 2898\mu mK \quad (4.2)$$

However, not only heated solids can be used as broad band emitters in the visible spectral range. Also *gas-discharge lamps* find use. Scattering of electrons and ions on neutral atoms in the plasma lead to a continuous broad band emission spectrum in the visible. The advantage of these gas lamps is the higher temperature that can be achieved. Typical representatives would be (*Quartz-*)*Halogen* lamps or *high pressure mercury* lamps.

### 4.1.2 UV light sources

As one can see from Fig. 4.1, the UV part of the spectrum of a black body emitter is rather low in intensity compared to the VIS/NIR part. Since the temperature necessary to shift enough intensity into the UV-range (Eqs. 4.1 and 4.2) are highly impractical, one has to come up with different solutions. In addition to the plasma emission, high pressure gas lamps exhibit narrow emission lines in the ultraviolet. They correspond to the fluorescence lines of the individual atoms. Typical emission spectra are shown in Fig. 4.2. In addition

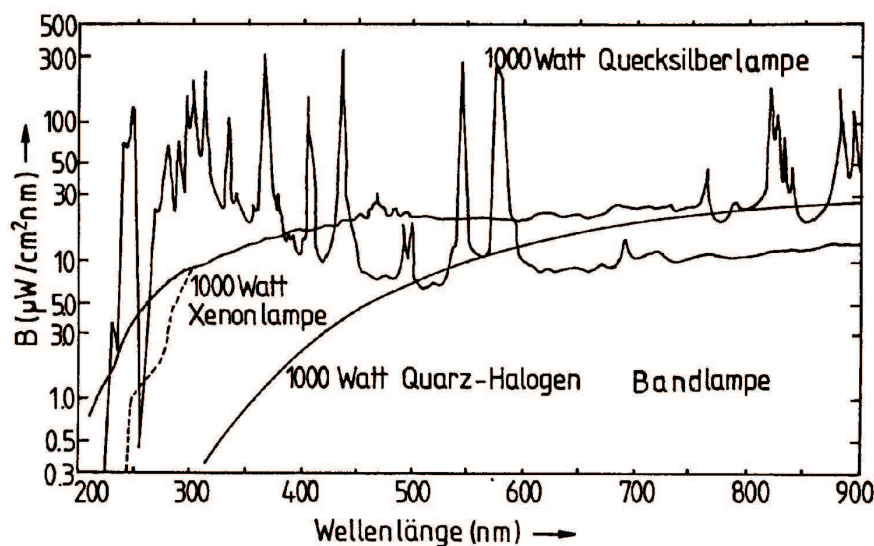


Figure 4.2: Emission spectra of typical UV light sources. For comparison the emission characteristic of a VIS broad band light source is also shown.

to the continuous broad band spectrum in the VIS region, sharp emission spikes in the UV are clearly visible. Mercury lamps, *Deuterium* lamps or *Xenon* lamps are typical representatives of this group of light sources.

## 4.2 Optical components

Between the main components of an optical setup, the light will be reflected, collimated, focused, etc. several times on its path from the light source through the sample to the detector. It will pass mirrors, windows and lenses. The optical properties of all these components need to be considered in our experimental setup.

### 4.2.1 Mirrors

In spectrometers one normally needs broad band mirrors with a high and possibly uniform reflectance over the whole UV/VIS/NIR range. The broad plasmon resonance (collective excitations of the quasi-free electrons) of highly conducting metals provides this optical response. Mirrors are often made from either polished metal surfaces, or a thin metal film is evaporated onto a suitable substrate. Note that the surface roughness of the metal needs to be significantly smaller than the wavelength of the reflected light in order to reduce scattering. A mirror that looks highly reflective to the eye (VIS) might be a good diffuse scatterer in the UV! A prototypical metal used for mirrors is *Al*, but also *Ag* is used. The reflectance for thin films of these metals is of course wavelength

Table 4.1: Reflectance  $R$  at wavelength  $\lambda$  of thin metal films deposited by vacuum evaporation.

Material	$R$	$\lambda$ [nm]
Ag	17.6	186.0
	18.9	208.0
	18.1	289.0
	34.3	360.0
	55.0	460.0
	57.2	560.0
	70.4	660.0
	75.5	690.0
Al	90.0	404.6
	91.5	491.6
	91.0	546.1
	90.0	578.0
	89.5	644.0

dependent. Some values are listed in Tab. 4.1.

### 4.2.2 Window, lenses, substrates, and sample cells

In the fabrication of transparent components for UV/VIS/NIR spectrometer one needs to take into account the fundamental absorption of the materials used. Ordinary glass as used for windows is not UV transparent. One has to resort to *Quartz glass* or *fused Silica* to ensure UV compatibility. In Fig. 4.3 the transmittance of several glasses used for transparent components in optical

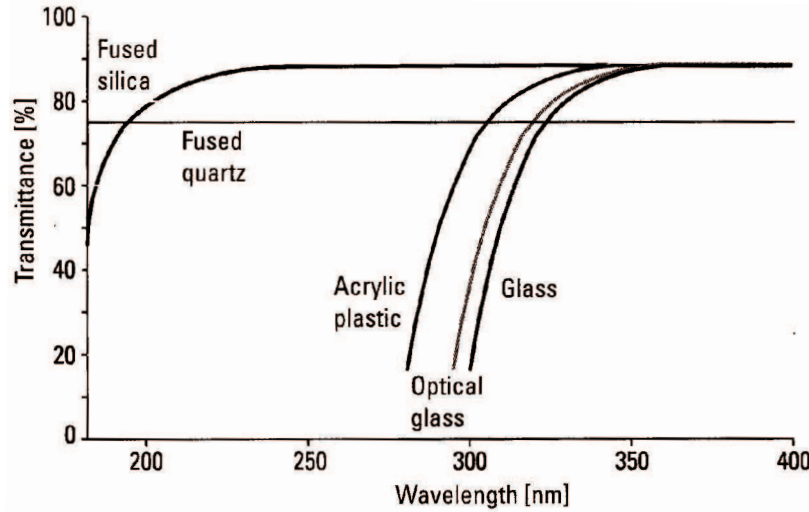


Figure 4.3: Transmittance as a function of wavelength of several glasses used for optical components (windows, lenses, etc.) in spectrometer setups.

setups is shown. Ordinary glasses are transparent up to  $\sim 300\text{nm}$ , while fused quartz and fused silica can be used up to  $\sim 200\text{nm}$ . Also diamond and sapphire ( $\text{Al}_2\text{O}_3$ ) can be used, the latter only as long as polarization does not need to be taken into account, since sapphire is birefringent.

### 4.3 Dispersive elements

The word *spectrometer* or *spectrograph* itself implies that the light is analyzed separately for each wavelength. Consequently, one needs to find a possibility to break down white light (from the light source) into its spectral components. Apart from interferometry there are two basic concepts how this is achieved in industrial solutions.

#### 4.3.1 Prisms

In Sect. 2.4 we have seen that the dielectric tensor  $\varepsilon$  and consequently the refractive index  $n$  is a function of the wavelength (see also Fig. 2.3, Tab. 2.1 and Eqs. 2.16 to 2.18). This is especially true in the vicinity of absorption features and internal resonances. This wavelength dependence is generally referred to as the *dispersion* of light in the medium. If the incident light has less energy than the fundamental electronic absorption, the refractive index is higher for shorter



wavelengths (=higher energies) as is shown in Fig. 2.3.

For light that passes through a prism with an opening angle  $\gamma$  in a totally symmetric configuration we find a total angle  $\delta$  of deflection:

$$\delta = -\gamma + 2 \arcsin \left( n \sin \left( \frac{\gamma}{2} \right) \right) \quad (4.3)$$

If we take a closer look at Eq. 4.3, we can see that, for a given geometry, blue light is deflected more than red light since  $\lambda_{red} > \lambda_{blue}$  and consequently  $n(\lambda_{blue}) > n(\lambda_{red})$ . The resolution of a prism spectrograph is given by:

$$\frac{\nu}{\Delta\nu} = b\nu^2 \frac{dn}{d\nu} \quad (4.4)$$

where  $\nu$  is the light frequency,  $b$  the base length of the triangular prism and  $dn/d\nu$  is the prism glass dispersion.

### 4.3.2 Gratings

A better resolution and a higher dispersion can be achieved by diffraction gratings. Since in transmission gratings most of the light intensity passes right through the grating and ends up in the zero<sup>th</sup> (undispersed) order, reflection gratings are used for all practical purposes. Additionally these reflection gratings are *blazed* for a certain wavelength and a certain order of diffraction to get even more intensity in that specific order. The resolution of a grating is given by:

$$\frac{\Delta\lambda}{\lambda} = \frac{1}{Nm} \quad (4.5)$$

where  $\lambda$  is the light wavelength,  $N$  the number of illuminated grates and  $m$  the order of diffraction. Furthermore, the resolution depends on the slit width used in the spectrometer setups. Generally gratings operate in first or second order. One has to keep in mind that  $\lambda = 350\text{nm}$  appears in second order at the very same angle as  $\lambda = 700\text{nm}$  appears in the first order. One also has to be aware of the fact that the performance of a grating in terms of total diffracted (reflected) intensity depends heavily on the polarization of the light with respect to the grating orientation (parallel or perpendicular to the grates). Note that in contrast to prisms, red light is deflected further than blue light.

## 4.4 Detectors

After having created the light, having sent it through the sample and after having it spectrally dispersed, one still needs to determine the light intensity at

a given wavelength. In order to accomplish this, two basic concepts are used. The *photo-effect* in photomultiplier tubes and *photoconduction* in semiconductor detectors.

#### 4.4.1 Photomultipliers

In order to exploit Einstein's photo-effect for light detection, one needs a three-step setup:

- **Photo-Cathode** Usually a plate of a low workfunction metal. This means that it does not take a lot of energy for a photon to kick an electron out of the bulk metal. Alkali metals or a mixture of alkali metals are used as photo-cathodes. If the light is too far in the red, the photons do not have enough energy to promote electrons out of the metal. In order to sensitize photomultiplier tubes in the red spectral region, the photo-cathodes can be covered by a thin layer of GaAs or some other low-bandgap semiconductor.
- **Dynodes** After the electron has been brought out of the cathode by incident light, it is accelerated towards a second metal plate, where it kicks out a whole bunch of secondary electrons. All these secondary electrons are then accelerated towards a third electrode and so on. After a cascade of several such electrodes (dynodes) one electron has become a veritable current pulse that finally impinges onto the
- **Anode.** The anode finally collects all these secondary electrodes and records the total current flowing through the photomultiplier. Without the photo-cathode the whole setup would be that of a *secondary electron multiplier* (SEM). Since the mean free path length of electrons on air is far too short, the whole described setup has to be mounted inside a vacuum tube, the so called *photomultiplier tube*.

The above described setup is schematically depicted in Fig. 4.4. The total voltage applied to the tube is in the range of several kV. In order to reduce the dark current through the device, photomultipliers are often cooled, for instance by Peltier elements. The material for the entrance window of the light has to be chosen depending on the wavelength range a specific tube is used for (see also Subsect. 4.2.2).

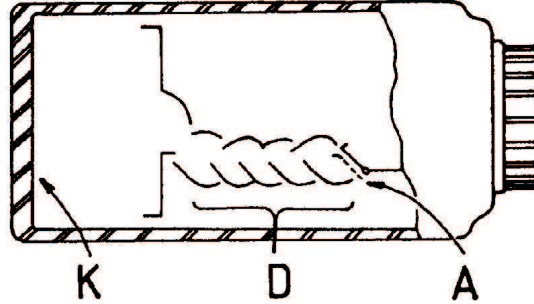


Figure 4.4: Schematic representation of a photomultiplier tube. Electrons are promoted out of the photocathode K by incident light, are then accelerated and multiplied by a cascade of dynodes D until they finally arrive at the anode A.

#### 4.4.2 Photoconduction detectors

The fact that incident, absorbed light (with energy greater than the bandgap) creates electron-hole pairs in semiconductors, can be used to measure light intensity. The more charge carriers are created inside a bulk semiconductor, the higher its intrinsic conductivity. The efficiency of charge carrier generation depends mostly on the absorption coefficient at a certain wavelength. We can see the link to the more theoretical chapter of this manuscript. Light is absorbed in the semiconductor, first a bound electron-hole pair is created, then the electron and the hole are pulled apart by an external electric field and lattice vibrations. Since semiconductors come with a broad variety of bandgaps (see Tab. 3.1, these detectors can be used over the whole UV/VIS/NIR range. In Fig. 4.5, the spectral sensitivity for photoconducting detectors made of a variety of semiconductors is shown.

Another possibility of using semiconductor devices for light detection is the *photodiode*. A semiconductor diode is biased in reverse direction. No current should flow. When one creates bound electron-hole pairs at the *np*-junction, the built-in field pulls them apart, free charge carriers are generated, and a photocurrent occurs in reverse direction that is proportional to the number of created electron-hole pairs and thus to the incident light intensity. In order for the light to access the interface between the two differently doped regions, one of them (either *n* or *p*) has to be made very thin, or more precisely, semitransparent. Very practical is the use of linear *photodiode arrays*, since the whole spectrum can be recorded at one shot instead of scanning it with exit slit. A photodiode array has to be read out in parallel mode. However, a specially crafted device of a linear arrangement of diode-like structures on one piece of

semiconductor material permits also a sequential readout of the whole spectrum. These detectors are called *charge coupled device* (CCD).

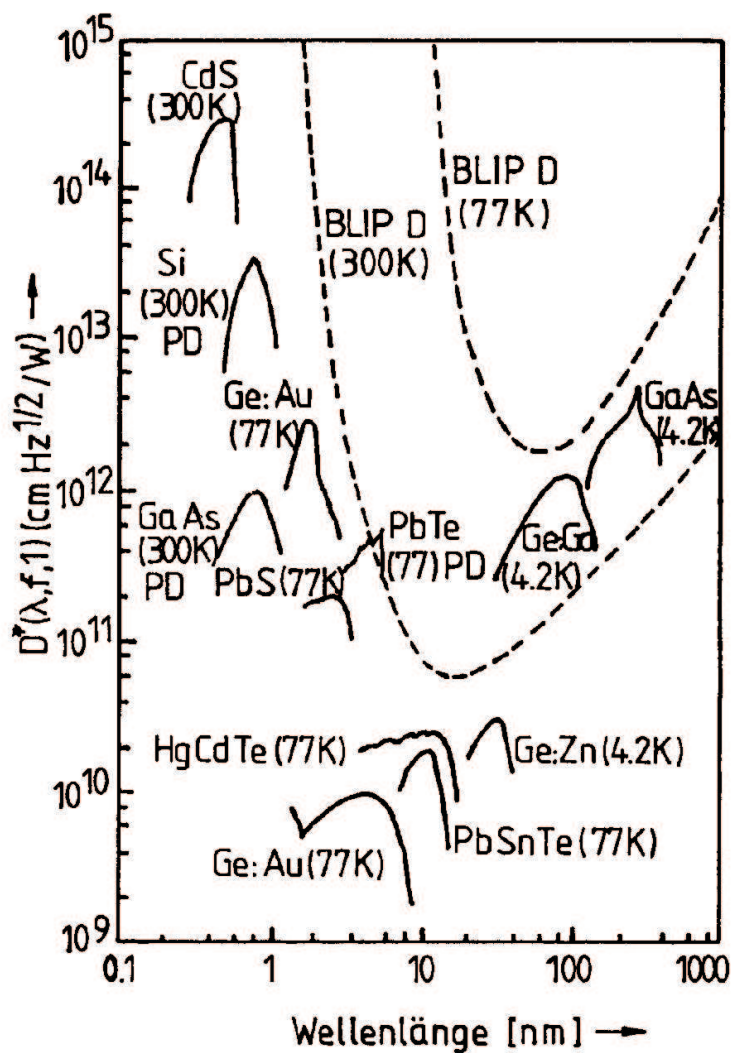


Figure 4.5: Spectral sensitivity of several important types of photoconducting semiconductor detectors.

# Bibliography

- [1] Hans Kuzmany, *Festkörperspektroskopie* (Springer, Berlin-Heidelberg-New York, 1989).
- [2] Bergmann Schaefer, *Lehrbuch der Experimentalphysik* **Vol 3**, Optik, 9. Auflage (Walter de Gruyter, Berlin-New York, 1993).
- [3] Helmut Vogel, *Gerthsen Physik*, 18. Auflage (Springer, Berlin-Heidelberg-New York, 1995).
- [4] Christian Weißmantel und Claus Hamann, *Grundlagen der Festkörperphysik*, 4. Auflage (Johann Ambrosius Barth, Heidelberg-Leipzig, 1995).
- [5] Eugene Hecht, *Optik* (Addison-Wesely, Deutschland, 1989).
- [6] George C. Schatz und Mark A. Ratner, *Quantum Mechanics in Chemistry* (Dover, New York, 2002).
- [7] Claude Cohen-Tannoudji, *Quantum Mechanics*, **Vol. 2**(John Wiley & Sons , New York-London-Sydney-Toronto, 1977).
- [8] Joseph R. Lakowicz, *Principles of Fluorescence Spectroscopy*, 2<sup>nd</sup> edition (Kluwer Academic/Plenum New York-Boston-Dordrecht-London-Moscow, 1999)